

Article

# Evidences of Different Drought Sensitivity in Xylem Cell Developmental Processes in South Siberia Scots Pines

Liliana V. Belokopytova <sup>1,\*</sup> , Patrick Fonti <sup>2</sup> , Elena A. Babushkina <sup>1</sup>, Dina F. Zhirnova <sup>1</sup> and Eugene A. Vaganov <sup>3,4</sup>

<sup>1</sup> Khakass Technical Institute, Siberian Federal University, 655017 Abakan, Russia; babushkina70@mail.ru (E.A.B.); dina-zhirnova@mail.ru (D.F.Z.)

<sup>2</sup> Swiss Federal Research Institute for Forest, Snow and Landscape Research WSL, CH-8903 Birmensdorf, Switzerland; patrick.fonti@wsl.ch

<sup>3</sup> Institute of Ecology and Geography, Siberian Federal University, 660036 Krasnoyarsk, Russia; eavaganov@hotmail.com

<sup>4</sup> Sukachev Institute of Forest, Siberian Branch of the Russian Academy of Science, 660036 Krasnoyarsk, Russia

\* Correspondence: white\_lili@mail.ru

Received: 23 September 2020; Accepted: 30 November 2020; Published: 30 November 2020



**Abstract:** *Research Highlights:* This study emphasized the importance of multi-parameter analyses along ecological gradients for a more holistic understanding of the complex mechanism of tree-ring formation. *Background and Objectives:* The analysis of climatic signals from cell anatomical features measured along series of tree-rings provides mechanistic details on how environmental drivers rule tree-ring formation. However, the processes of cell development might not be independent, limiting the interpretation of the cell-based climatic signal. In this study, we investigated the variability, intercorrelations and climatic drivers of wood anatomical parameters, resulting from consequent cell developmental processes. *Materials and Methods:* The study was performed on thin cross-sections from wood cores sampled at ~1.3 m stem height from mature trees of *Pinus sylvestris* L. growing at five sampling sites along an ecological gradient from cold and wet to hot and dry within continental Southern Siberia. Tracheid number per radial file, their diameters and wall thicknesses were measured along the radial direction from microphotographs for five trees per site. These parameters were then averaged at each site for earlywood and latewood over the last 50 tree rings to build site chronologies. Their correlations among themselves and with 21-day moving climatic series were calculated. *Results:* Our findings showed that wood formation was not simply the result of environmentally driven independent subprocesses of cell division, enlargement and wall deposition. These processes appear to be interconnected within each zone of the ring, as well as between earlywood and latewood. However, earlywood parameters tend to have more distinctive climatic responses and lower intercorrelations. On the other hand, there are clear indications that the mechanisms of cell division and enlargement share similar climatic drivers and are more sensitive to water limitation than the process of wall deposition. *Conclusions:* Indications were provided that (i) earlywood formation left a legacy on latewood formation, (ii) cell division and enlargement shared more similar drivers between each other than with wall deposition, and (iii) the mechanism of cell division and enlargement along the gradient switch from water to heat limitations at different thresholds than wall deposition.

**Keywords:** quantitative wood anatomy; tracheid radial diameter; cell wall thickness; earlywood; latewood; ecological gradient

## 1. Introduction

Trees, due to their longevity and their environment-sensitive annual increments, are excellent biological sensors to retrospectively assess environmental changes. Tree-ring width is commonly used for such reconstruction since it is easy to measure on softwoods and in porous ring hardwoods [1,2] and it adequately integrates the biologically relevant climatic signal. Since tree growth is primarily driven by light, temperature and water availability [3,4], tree rings proved helpful for reconstructing local climate (e.g., [5,6]).

In recent years, dendrochronology has evolved including more tree-ring traits which are helping to better understand the causal relationships between environmental factors and tree performance ([7–10], etc.). Among them, wood anatomy is one of the subdisciplines that provides novel contributions. Quantitative wood anatomy, i.e., the use of intra-annually resolved wood cell anatomical characteristics along dated tree-ring series [2,11,12], effectively complements the information obtained from tree-ring width. A first important advantage is the increased temporal resolution of the climatic response encoded in cells [13–15], environmentally-sensitive formation of which occurs over only few weeks [16,17]. A second benefit is related to the diversity of anatomical parameters (such as the number, size and wall thickness of tracheids in conifers) representing corresponding cell development processes (cell division, enlargement and secondary wall deposition), which respond to different environmental factors [4,18]. Another advantage of quantitative wood anatomy is the strong link between structure and function in xylem as a tissue. In conifers, where tracheids play different roles depending on their position in the ring, cell wall thickness and tracheid radial diameter assume different functional meanings [14,19], which can be used to interpret the environmental impact on xylem functional performance. Specifically, earlywood tracheid traits are closely linked with the xylem hydraulic properties, while the latewood cell wall thickness is a rather reliable proxy of mechanical properties and carbon fixation in wood [20–22].

Despite the more mechanistic and functional interpretation offered by quantitative wood anatomy, this approach has not considered restrictions imposed on environmental signals by the cell production chain. Since wood formation is a gradual proliferation of xylem cells in which phases of cell production and differentiation are separated in space and time during the growing season, one can expect that it is possible to independently identify the environmental factors constraining each developmental process of each single cell produced over the full growing season [23]. However, these developmental processes might not be fully independent from each other, since cells generated by the cambium follow a strict production line through cell developmental processes that run in parallel. While some cells undergo cell wall deposition, others (generated later) are still enlarging or dividing. Thus, what occurs at a certain cell developmental stage might depend on what has happened during the previous stages. It might eventually result in the constrained relations between parameters (e.g., that wall thickness depends on cell diameter) or between ring sectors (that latewood characteristics depend on earlywood ones) hindering the interpretation of the environmental signal.

In this study, we aim at exploring these relations by performing quantitative cell anatomical measurements along series of tree-rings to (i) quantify correlations among cells' anatomical parameters and between cells formed at different seasons to (ii) investigate their response to climatic variability. This study is performed on an ecologically tolerant and widespread coniferous species, Scots pine (*Pinus sylvestris* L.) [24,25], at five sites along an ecological gradient ranging from thermal to water limitations that also accounts for the diversity of environmental conditions.

## 2. Materials and Methods

### 2.1. Study Area and Site Selection

The study was performed on five sampling sites in southern Siberia, Russian Federation (Table 1, Figure 1). Four sites were distributed along an elevation gradient from the lower part of taiga belt at 500 m a.s.l. up to the forest line at 1350 m a.s.l.

**Table 1.** Description of sampling sites and climatic stations (climatic data averaged over 1964–2014).

Site/Station	Coordinates			Slope		Forest Composition <sup>1</sup>	Average Climate (May–Sep)		
	Lat. (°N)	Long. (°E)	Elev. (m a.s.l.)	Aspect	Angle (°)		Temp (°C)	Prec. (mm)	Radiation (kW/m <sup>2</sup> )
ShB_1300N	52.809	91.507	1350	NE	25–30	PISI PISY PCOB	8.2	1390	600
ShB_900N	52.840	91.451	950	N	25–30	PISY LASI ABSI PPTM	10.8	990	600
ShB_900S	52.839	91.450	950	S	30–35	PISY LASI PPTM	10.8	990	770
ShB_500S	52.827	91.448	550	S	20–25	PISY LASI PPTM	13.4	590	730
MIN_300	53.723	91.867	300	flat	0	PISY BEPE	14.9	260	670
Cheryomushki	52.87	91.42	330	E	< 10	–	14.7	390	660
Minusinsk	53.68	91.67	250	flat	0	–	15.2	260	670

<sup>1</sup> Species codes are given according to the list of species used in tree-ring research ([26]): ABSI, *Abies sibirica* Ledeb.; BEPE, *Betula pendula* Roth.; LASI, *Larix sibirica* Ledeb.; PCOB, *Picea obovata* Ledeb.; PISI, *Pinus sibirica* Du Tour; PISY, *Pinus sylvestris* L.; PPTM, *Populus tremula* L.

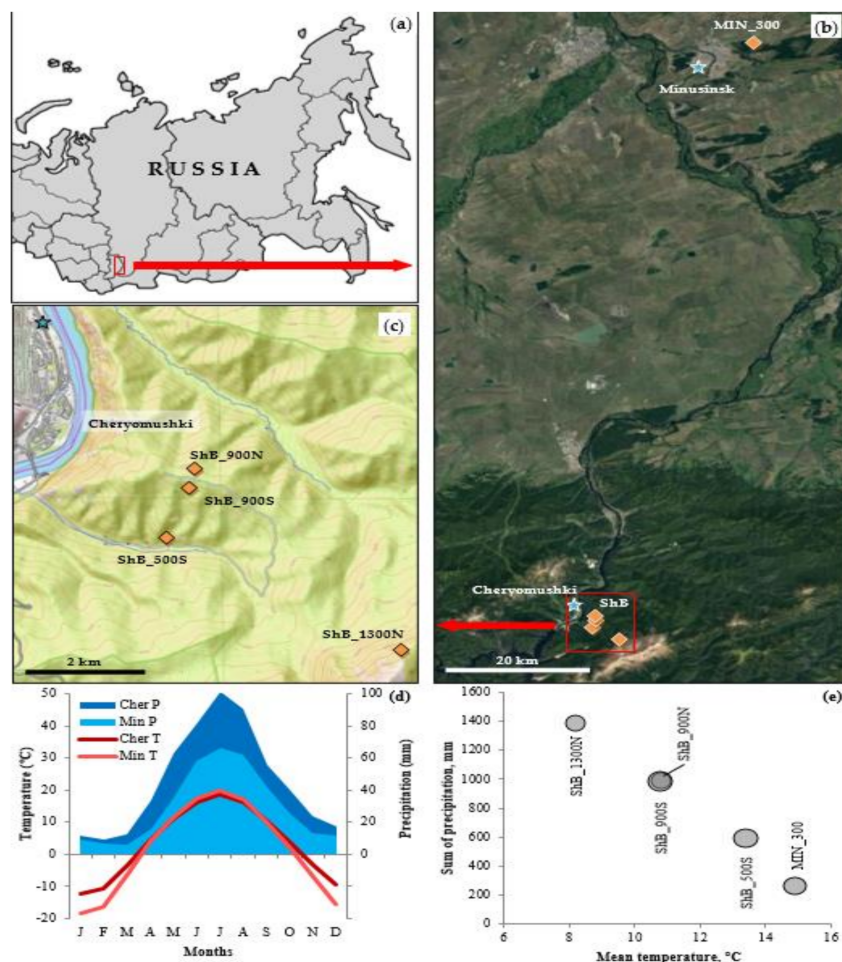


**Figure 1.** Study area with selected sites: (a) Location of the study area within the Asian part of Russia; (b) location of the sampling sites (diamonds) and climatic stations (stars) within the study area; (c) topographical map of the four sites in the Shushensky Bor; (d) climatic diagrams (1964–2014) at the climatic stations of Cheryomushki (Cher) and Minusinsk (Min); (e) location of the sites within the temperature vs. precipitation plot (May–September; see Table 1) to illustrate the ecological gradient considered in the study; the size of circle is proportional to the received solar radiation.

These sites were located in the National park “Shushensky Bor” in the Western Sayan Mountains within 10 km from the Cheryomushki climatic station (330 m a.s.l.). An additional site (about 100 km north from the previous ones) was located on a flat plain at 300 m a.s.l. in a dry pine forest named Minusinsky Bor within the steppes of the Khakass-Minusinsk Depression. This site distanced 9 km from the Minusinsk climatic station (250 m a.s.l.).

The climate of the region is sharply continental [27], characterized by large daily and seasonal temperature variation and by uneven seasonal distribution of precipitation. According to 1964–2014 records ([www.meteo.ru](http://www.meteo.ru)) from the climatic stations of Cheryomushki and Minusinsk, the mean annual temperature and precipitation are 1.6 and 3.6 °C, and 354 and 541 mm, respectively (Figure 1d). Precipitation is falling mainly during the warm season. In Cheryomushki, at the foothills of the elevational gradient, the average temperatures of the warm season (April–October) are  $11.7 \pm 0.7$  °C and the total precipitation sum is  $460 \pm 80$  mm (mean  $\pm$  standard deviation). The local temperature lapse rate during the warm season is ca. 0.65 °C per 100 m of elevation, whereas annual precipitation increases by 100–200 mm per 100 m [28]. In comparison to Cheryomushki, the climate of Minusinsk is slightly more continental and much drier; in April–October average temperature is  $11.7 \pm 0.6$  °C, and the precipitation sum is  $310 \pm 60$  mm.

The forests of the region are usually dominated by the coniferous *Pinus sylvestris* L., *Pinus sibirica* Du Tour, *Larix sibirica* Ledeb., *Picea obovata* Ledeb., *Abies sibirica* Ledeb.; deciduous *Betula pendula* Roth. and *Populus tremula* L. also occur at lower elevations. Soils in mountains around Cheryomushki are in general loamy, thin, and stony with numerous hard rock outcrops but the depth and fertility can strongly vary depending on the local landscape. In Minusinsky Bor, soils are sandy and contain ca. 7–10% of humus in the upper 8–10 cm layer.

The sites were selected along an elevation gradient to cover a water stress gradient ranging from cold and wet (warm season means are 8.2 °C and 1390 mm) to warm and dry (15.2 °C and 260 mm) (Figure 1e, Table 1), considering a lapse rate of +100 mm of May–September precipitation and  $-0.65$  °C of May–September temperature for every 100 m rise in elevation referenced to the measured values from the closest climatic stations. Additionally, to also account for contrasting solar radiation, the south-facing 900 m a.s.l. elevation site was contrasted with a site on the same elevation but the opposite slope. The solar radiation was estimated using the ArcGIS software ([www.esri.com](http://www.esri.com)) based on the SRTM v3 digital terrain model. Obviously, there is substantial uncertainty in climatic characteristics at the sampling sites, but it does not change principal pattern of ecological gradient.

## 2.2. Tree-Ring and Cell Anatomical Measurement

Stem wood cores from at least 20 mature and dominant *Pinus sylvestris* trees without visible damages were collected from each site. Sample collection was performed at 1.3 m stem height using a 5-mm increment borer. After core surface preparation, the tree-ring width (TRW) of all annual rings of each core has been measured with a LINTAB measuring table using the TSAPwin software (Rinntech, Germany). Tree-ring width time-series were visually and statistically cross-dated according to standard dendrochronology methods [29].

Cell anatomical measurements were performed on the last 50 annual rings (for the period 1965–2014 at the ShB sites and 1964–2013 at the MIN site) on a selection of five trees per site (Figure A1 in Appendix A). For the selection, we considered the trees with ring-width time-series that showed the highest correlations to the mean site chronology and which were at least 80–120 rings long to ensure a representative site signal and minimize age-trend effects [30]. Cell measurements were performed on images from 15–20  $\mu$ m thick cores' cross-sections (Figure A2 in Appendix A). Cross-sections were obtained from the water-soaked softened cores using a sledge microtome (Microm HM 430, Thermo Fisher Scientific, USA), then stained with safranin, dehydrated with increasing concentrations of ethanol solutions, washed with xylol, and permanently preserved in Canada balsam. Images were captured using a digital camera connected to a microscope (AXIOCam MRc5, Axio Imager D1, Zeiss, Berlin, Germany) with a resolution of 3.7 pixels per micron. Anatomical measurements on the dated

tree rings were performed using the program Lineyka [31]. For each ring, we measured the lumen diameter ( $LD$ ) and the double cell wall thickness ( $2CWT$ ) in the radial direction along five radial files of tracheids [32,33] with an accuracy of  $0.01 \mu\text{m}$ . The program ProcessorKR [31] was used to derive the radial diameter  $D = LD + 2CWT$  of each single tracheid along the radial file to obtain tracheidograms, which were then standardized to the mean number of cells per ring and averaged over 5 radial files [34].

The separation between earlywood and latewood cells has been performed according to Bryukhanova and Fonti [35], i.e., by defining site-specific threshold values  $k$  that best separate the kernel density maxima in the bimodal distribution of the ratio between cell wall thickness and tracheid diameter ( $CWT/D$ ). Specifically, tracheids showing a  $CWT/D < k$  were assigned to earlywood, with the exception of the small amount of intra-annual density fluctuations (IADF) where latewood-type tracheids forming within the earlywood were still considered as earlywood tracheids (Figure A3 in Appendix A). Cell number, mean tracheid diameter, and mean cell wall thickness were then calculated accordingly for earlywood and latewood of each ring.

### 2.3. Tree-Ring Chronologies, Correlation Matrices, and Climate–Growth Relationships

Cell anatomical time-series of earlywood and latewood  $N$ ,  $D$ , and  $CWT$  were averaged into site chronologies. These parameters were selected as indicators of the processes of cell division ( $N$ ), cell enlargement ( $D$ ), and wall-deposition ( $CWT$ ). No detrending of the cell anatomical time-series was performed, since their changes related to tree size and age have already been minimized by omitting the juvenile wood from the time-series [30,33,36,37]. The strength of the common signal in site chronologies has been quantified for each site and parameter using the mean inter-series correlation between the time-series of the five individual trees. One-way ANOVA was used on site chronologies (i.e., the highest level of data hierarchy) to determine the significance of site differences between mean values of each anatomical parameter. To estimate the significance of differences between each pair of site chronologies, the Tukey post-hoc test was applied.

Matrices of paired Pearson correlations within each parameter at different sites and between parameters within each site have been performed to investigate how the parameters' association varies along the ecological gradient. Significance of correlations was evaluated with a  $t$ -test; a level of significance of  $p < 0.05$  was used. The climatic signal in anatomical parameters has been calculated by paired Pearson correlations between the site chronologies of each parameter and the series of temperature and precipitation from 1964 to 2014, calculated from daily data using a 21-days window moving in daily steps over the growing season, i.e., from May to September.

For all these analyses, we applied linear models as this approach has already been successfully applied for various long-term anatomical datasets, both in terms of interrelations between chronologies and climate–growth relationships (e.g., [14,15]).

## 3. Results

### 3.1. Characteristics of Site Chronologies

The 50-yr long site raw chronologies showed a rather flat linear trend over time except for the cell number for the ShB\_900S site (Figure 2). The cell diameters and the latewood cell walls were relatively stable along the gradient (Figure A4 in Appendix A). Cell numbers tended to be lower at the extremes of the gradient, but clearly increased with site temperature while opposite trend was observed for the wall thickness of the earlywood cells. The coefficient of variation, despite it being double for  $N$  (15–27%) than for  $D$  and  $CWT$  (2–12%), was relatively stable along the gradient (Figure 2, Figure A5 in Appendix A). The common signal (here assessed as mean inter-series correlation) was higher for  $N$  (up to 0.50) than for  $D$  (up to 0.37) and  $CWT$  (up to 0.27) with correlations ranging from 0.1 to 0.5 depending on the parameter and site (Table 2). The common signal was among the strongest at the extremes of the ecological gradient: for  $TRW$ ,  $N$ , and  $CWT$ , the signal was strongest at the wettest and coldest site, while  $D$  showed the strongest agreement among trees at the warmest and driest

site. Moreover, the sites ShB\_900N and ShB\_900S, despite their close location and similar elevation, showed important differences in the strength of the signal for *N* and *D*.

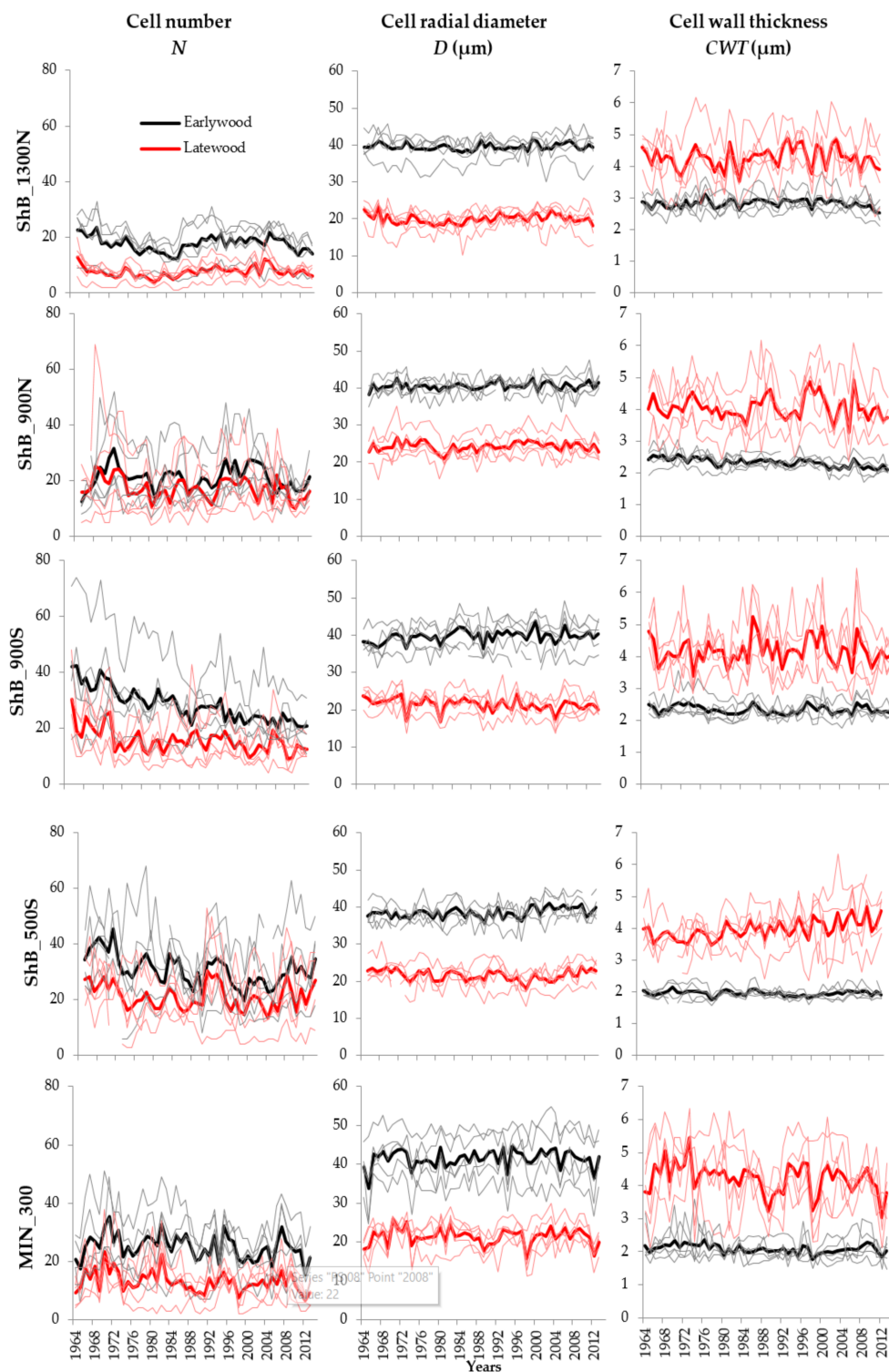


**Figure 2.** Overview of all Scots pine raw chronologies grouped by site and tree-ring parameter. Thin lines represent series of individual trees; thick lines represent site average chronologies.

**Table 2.** Mean inter-series correlations of Scots pine cell anatomical chronologies. For comparison, values for tree-ring width chronologies of the same sites standardized using 67% cubic spline [29] are shown.

Parameters <sup>1</sup>	Site				
	ShB_1300N	ShB_900N	ShB_900S	ShB_500S	MIN_300
<i>TRW<sub>site</sub></i>	<b>0.48</b> <sup>2</sup>	0.27	0.30	0.28	0.27
<i>TRW<sub>5</sub></i>	<b>0.50</b>	0.25	0.39	0.27	0.28
<i>New</i>	<b>0.47</b>	0.24	0.33	0.25	0.23
<i>Nlw</i>	<b>0.49</b>	0.24	0.41	0.23	0.31
<i>Dew</i>	0.16	0.12	0.27	0.16	<b>0.37</b>
<i>Dlw</i>	0.19	0.13	0.38	0.10	<b>0.36</b>
<i>CWTew</i>	0.10	<b>0.18</b>	0.10	0.10	0.09
<i>CWTlw</i>	0.25	<b>0.27</b>	0.17	0.16	0.18

<sup>1</sup> *TRW<sub>site</sub>* = site chronology of tree-ring width based on all sampled trees; *TRW<sub>5</sub>* = site chronology of tree-ring width based only on five trees selected for anatomical measurements; *New* = number of cells in earlywood; *Nlw* = number of cells in latewood; *Dew* = average cell radial diameter in earlywood; *Dlw* = average cell radial diameter in latewood; *CWTew* = average cell wall thickness in earlywood; *CWTlw* = average cell wall thickness in latewood. <sup>2</sup> Values in bold indicate the maximum common signal strength along the ecological gradient for a given parameter.

### 3.2. Correlations Within and Between Parameters

The correlation matrices for the same parameter across different sites showed relatively few significant correlations (Figure 3). Positive significant correlations ( $p < 0.05$ ) were observed for earlywood parameters between the most drought-exposed sites (MIN\_300, ShB\_500S and ShB\_900S) and in the latewood parameters between the ShB\_900 sites. The only negative significant relationships were observed for *Dew* among the colder and wetter sites.

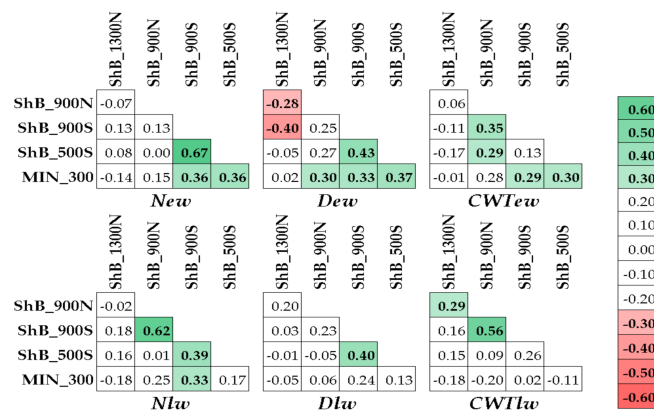


**Figure 3.** Between-site correlation matrices grouped by cell parameter. Colors indicate significant correlations at  $p < 0.05$ .

The correlations between parameters of the same site were very variable (Figure 4). These were ranging from a minimum of -0.23 for *New* × *Dew* at ShB\_900S to a maximum of 0.79 for *Dlw* × *CWTlw* at MIN\_300, and were generally stronger between the earlywood and latewood values of the same parameter (i.e., within the *N*, *D* and *CWT* types) and weakest between successive stages of tracheid differentiation in earlywood (*New* and *Dew*, *Dew* and *CWTew*). When considering their variations along the ecological gradient, it has been possible to identify distinct patterns. The first pattern was characterized by constantly positive significant correlations with the highest values at the extremes. So, for example, the correlation between *Dlw* and *CWTlw* was constantly positively significant, with the highest values at MIN\_300 ( $r = 0.70$ ) and ShB\_1300N ( $r = 0.79$ ). The second pattern grouped correlations that did not show a clear trend along the gradient. For example, the correlation between *New* and *Nlw* was moving within a relatively small range between 0.44 and 0.67 at all sites. The third pattern was

characterized by correlations showing a clear change in sign from positive at the extremes to negative in the center of the gradient.

	ShB_1300N	ShB_900N	ShB_900S	ShB_500S	MIN_300	
<i>New x Dew</i>	0.33	0.19	-0.23	0.04	0.57	Earlywood
<i>New x CWTeW</i>	0.14	0.06	0.32	0.18	0.25	
<i>Dew x CWTeW</i>	0.11	-0.11	0.21	0.10	0.01	
<i>Nlw x Dlw</i>	0.77	0.39	0.61	0.51	0.76	Latewood
<i>Nlw x CWTeW</i>	0.70	0.46	0.45	0.28	0.64	
<i>Dlw x CWTeW</i>	0.70	0.40	0.55	0.27	0.79	
<i>New x Nlw</i>	0.60	0.44	0.61	0.67	0.62	Same type of parameter
<i>Dew x Dlw</i>	0.29	0.28	0.39	0.22	0.48	
<i>CWTeW x CWTeW</i>	0.65	0.35	0.55	0.24	0.48	
<i>New x Dlw</i>	0.64	0.43	0.43	0.72	0.61	Other combinations
<i>New x CWTeW</i>	0.39	-0.01	0.10	-0.18	0.54	
<i>Dew x CWTeW</i>	0.10	0.05	0.47	0.52	0.45	
<i>Nlw x Dew</i>	0.11	-0.09	-0.10	0.08	0.26	
<i>Nlw x CWTeW</i>	0.40	0.40	0.48	0.25	0.34	
<i>Dlw x CWTeW</i>	0.33	0.18	0.44	0.39	0.33	

**Figure 4.** Between-parameter correlations along the ecological gradient. Colors indicate significant correlations at  $p < 0.05$ .

### 3.3. Climate–Growth Relations

The sites at the extremes of the ecological gradient generally showed contrasting responses to climate, independently from the investigated cell anatomical parameters (Figure 5). At the cold and wet forest-line ShB\_1300N site, anatomical parameters for most of the growing season positively responded to temperature and negatively to precipitation, whereas it was the opposite for the dry and warm MIN\_300 site. For the sites in the central part of the gradient, the climatic response was often in between these two types. It was also possible to observe a tendency for an earlier temperature signal in the earlywood chronologies than for the latewood ones. This pattern was, however, less pronounced for the responses to precipitation where, in addition to a similar signal as for the earlywood, a second climatic signal appeared later in the summer.

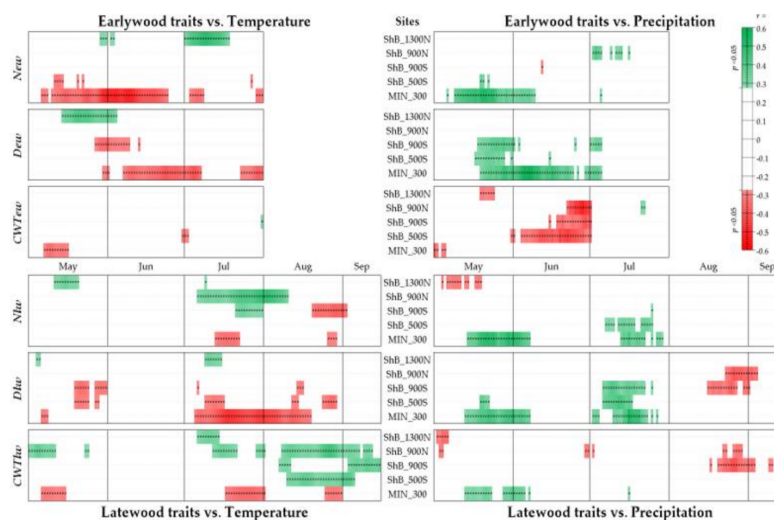


**Figure 5.** Correlations between earlywood (top) and latewood (bottom) cell anatomical chronologies with the 21-day moving series of mean temperature (left) and precipitation (right). Strength of positive (green) and negative (red) correlations (only significant at  $p < 0.05$ ) is represented by intensity gradient of color, see the legend. Version representing all correlations including those not significant at  $p < 0.05$  is showed as Figure A6 in Appendix A.

In regard to the earlywood (Figure 5, upper panels), at all elevations, climate affected the anatomical parameters from approximately the beginning of May to July 20. The temperature signal in general tended to peak on later date as the heat supply increased; this trend was especially pronounced for *Dew* and almost not existent for *CWTew*. Temperature limitation (i.e., positive signal to temperature) was observed only at the upper forest line, while at the other sites the negative signal to temperature was coupled to a positive precipitation signal, indicating drought stress. Despite the weak climatic response in *CWT*, in contrast to the other parameters, there was a slight tendency to a negative response to precipitation at all sites except MIN\_300.

In latewood (Figure 5, lower panels), the climatic influence on cell production was also observed since May, but extended at all sites until the first half of August with a break around June to the beginning of July, depending of the site. In the cell radial diameter, the climatic effect was most pronounced in July and the first half of August, although the influence of previous conditions was also observed. The temperature limitation of latewood cell formation reached lower elevations than for earlywood, being negative and decoupled from a positive precipitation signal (drought signal) for all the sites below ShB\_900N. In addition, *N* and *D* also negatively responded to a warm and wet August. For *CWT*, a positive influence of summer temperatures and negative one of precipitation was observed at all Shushensky Bor sites. However, in the Minusinsky Bor, all parameters showed a similar climatic response.

#### 4. Discussion

The conifer tree-ring anatomical structure is the result of individual tracheids sequentially moving through a defined chain of parallel running developmental processes (cell division, enlargement, and wall thickening) [23] that shares the same resources (assimilates; see [38]) and constraints (e.g., abiotic factors as heat and moisture). The main source for cell ecological information results from how these requirements and constraints differently interact to shape the observed variability of the tree-ring structure [39–41]. To identify common drivers across the complex cell formation machinery, in this study we assessed similarities and climatic responses of developmental-specific tracheid anatomical characteristics of the earlywood and latewood (number of cells = cell division, cell diameter = enlargement; and cell wall thickness = secondary wall deposition), and how these interlinked variabilities change along a large regional ecological gradient.

##### 4.1. Variabilities and Their Drivers

The three anatomical cell parameters considered (namely the number of cells *N*, the average cell diameter *D* and the average cell wall thickness *CWT*) displayed different inter-annual variation, whereby the cell size parameters (*D* and *CWT*) showed much lower coefficient of variations than *N* (Figure A5 in Appendix A). These coefficients were also lower for the earlywood parameters compared to the latewood ones. Such differences in the year-to-year variation support previous observations of a reduced variability in the morphology of earlywood tracheids which have to follow more strict biophysical constraints [42] in accordance to the size of the tree [36,37] to secure the essential function of an efficient and safe water transport [21,43]. On the contrary, the variability of the cell number is not limited functionally but might instead simply be a passive indicator of yearly or seasonal performance of cambial division. Despite these differences in constraints, some parameters still showed a certain common year-to-year variability (Figure 4). For example, the strong correlations between earlywood and latewood for the same parameters were mostly significantly positive ( $0.65 > r > 0.22$ ) suggesting that, with slight differences among sites, the earlywood and latewood parameters share some common driver. This common signal is related to the same response to climatic conditions that occurred prior and/or during the formation of the earlywood. Such relations well confirm established observations for intra-annual density showing that, except for very high latitudes ( $>60^\circ$ , where the growing season is quite short), latewood density encodes both spring (in common to the earlywood) and summer temperature signals [44]. Interestingly, similar common variabilities are also observed between

different parameters across the whole gradient, both within (e.g., among all latewood parameters) and between the sectors (e.g., between the *New* and the *Dlw* or *CWTew* and *Nlw*). Some of these relationships were also modulated by the environmental conditions where the correlations became significant only under extreme conditions, i.e., at both extremes of the gradient ( $New \times CWTlw$  or  $New \times Dew$ ) or under the more drought exposed conditions ( $Dew \times CWTlw$ ). We interpret these shared variabilities among parameters as indications of dominant common environmental drivers influencing the different processes shaping the ring structure. From our results, it emerges that, despite the link between earlywood and latewood, the processes involved in the formation of the latewood cells are—with different weight—mostly dominated by the same environmental constraint, namely summer drought. This is confirmed from the climate–growth correlations which show a general pattern at almost all sites, specifically that latewood parameters have a strong July–August response to temperature, precipitation, or both (Figure 5). The sign of the correlations depends on the mechanism shaping the considered parameter. Temperature and precipitation favor cambial division at the sites where the respective factor is most limiting tree growth [14,45], while the cell size mostly depends on turgor pressure [46–49] and thus at the drought-prone sites is promoted by cold and wet conditions [50,51]. Finally, the wall thickening (an important component in determining latewood density) mostly depends on the deposition of available carbon assimilates, a process primarily dependent on summer temperatures [20,44,52,53]. The picture is more complex when considering the climatic responses of the earlywood cell parameters, since the different cell developmental stages seem to be more independent in the response to the environmental parameters. The fact that the climatic signals of the three developmental processes are coherently temporally shifted along the production chain (division, enlargement, wall thickening) might already explain the lower agreement among the earlywood parameters. Nevertheless, the strong correlations between the number and size of earlywood cells, at least for the extremes of the gradient, might be explained by the fact that both processes respond to the same factor during approximately the same period.

#### 4.2. Variation of Climatic Responses along the Gradient

The wood anatomical responses were very changeable along the ecological gradient. In some cases, the climatic signal of a given parameter changed from positive to negative, especially for the response to temperature. The correlation matrices among the same parameters between sites (Figure 3) clearly support the hypothesis that positively significant similarities between sites are mostly limited to the ecologically closest sites.

Comparison of the spatial and temporal (during the season, in accordance with the timing of the corresponding xylogenesis phases for earlywood and latewood) changes in the climatic response of the selected parameters showed different sensitivity of the parameters along the ecological gradient. Although it appears to be clear that there was a switch from moisture availability to heat supply for the onset of the vegetative season along the ecological gradient, the climatic response in *New* and *Dew* is already shifting towards the limitation by heat supply at an altitude of 900 m a.s.l., while this switch is closer to 500 m a.s.l. for *CWTew*. From this comparison, it also emerges that *CWTlw* is largely limited by temperature throughout the entire pine distribution range except for the most dry and hot MIN\_300 site, while the more turgor-related mechanism of cell enlargement (*Dlw*) is sensitive to water deficit below 900 m a.s.l. These results indicate that threshold of the switch from water to heat limitations for the mechanism of cell division and enlargement is decoupled from wall deposition, which is less sensitive to drought.

## 5. Conclusions

This study on *Pinus sylvestris*, performed along a large ecological gradient, provides indications that wood formation is not simply the result of independent sub-processes of cell division, enlargement and wall deposition. This study provided initial indications that (i) earlywood formation can leave a legacy on latewood formation, (ii) cell division and cell enlargement share more similar drivers than

with wall deposition, and (iii) the mechanism of cell division and enlargement switch from water to heat limitations at different thresholds than for wall deposition. On the one hand, our results suggested that the processes occurring in the latewood are not independent from the ones occurring during the formation of the earlywood, and that earlywood parameters tend to have more distinct responses since the processes are more clearly separated in time than for the latewood parameters. On the other hand, there are clear indications that the mechanisms of cell division and enlargement share similar drivers and that they are more sensitive to water limitation than the process of wall deposition.

It can therefore occur that the ongoing global warming causes impairment between these mechanisms, inducing the formation of smaller cells with thicker walls. This might eventually cause the formation of a denser wood with less effective water transport, which will also induce smaller trees. Future research in natural conditions or greenhouse/field experiments could be addressed to further verify these observations in other species and/or environments and to investigate the consequences for wood growth and water transport in trees to estimate their impacts on forest ecosystem services.

**Author Contributions:** Conceptualization, E.A.V.; methodology, E.A.V.; validation, E.A.B. and E.A.V.; formal analysis, L.V.B. and P.F.; investigation, D.F.Z.; resources, E.A.B. and D.F.Z.; data curation, L.V.B.; writing—original draft preparation, L.V.B., D.F.Z. and P.F.; writing—review and editing, L.V.B., D.F.Z., E.A.V., and P.F.; visualization, L.V.B.; supervision, E.A.V.; project administration, E.A.B. and D.F.Z.; funding acquisition, E.A.V. All authors have read and agreed to the published version of the manuscript.

**Funding:** This research was performed within the framework of a state assignment of the Ministry of Science and Higher Education of the Russian Federation (FSRZ-2020-0010); the study was funded by the Russian Foundation for Basic Research, grant number 19-04-00274; and the Russian Science Foundation, grant number 19-18-00145.

**Acknowledgments:** The authors are grateful to the administration and employees of the National Park “Shushensky Bor” for permission to conduct research in the park territory and assistance in organizing field work.

**Conflicts of Interest:** The authors declare no conflict of interest. The funders had no role in the design of the study; in the collection, analyses, or interpretation of data; in the writing of the manuscript, or in the decision to publish the results.

## Appendix A

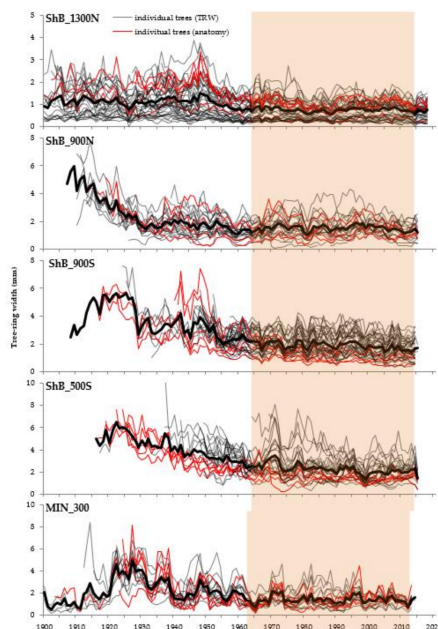


**Figure A1.** Tree-ring width raw time series at each sampling site (for ShB\_1300N part of the plot before 1900 was cut off). Thick lines represent averaged site chronologies; thin lines represent series of individual trees; series of trees selected for wood anatomy are marked with red color. Shaded area marks periods of anatomical measurement.

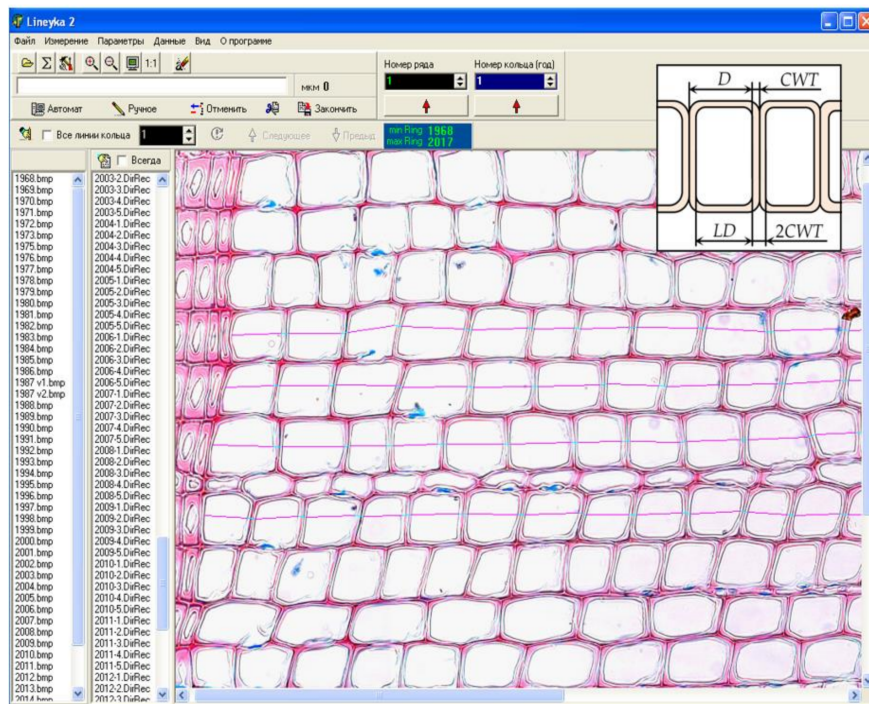


**Figure A2.** Measurement of Scots pine wood anatomical parameters on the microphotography with the Lineyka 2.0 program [32]. Lines on the photo are paths of measurement along radial files of tracheids; for each path result of measurement is a consequence of lumen diameter ( $LD$ , cyan segments of lines) and double cell wall thickness ( $2CWT$ , magenta segments) values. Inset shows the scheme of initially measured parameters ( $LD$  and  $2CWT$ ) and parameters calculated from them in the ProcessorKR program (radial cell diameter  $D$  and single cell wall thickness  $CWT$ ) [32].

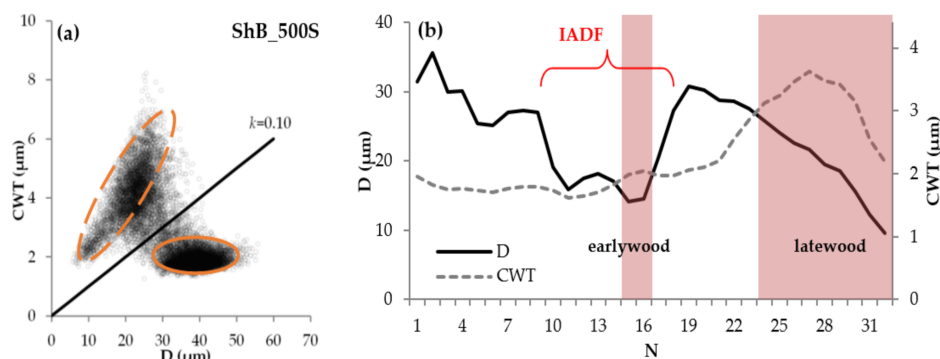


**Figure A3.** Procedure of separating earlywood and latewood: (a) dependence of  $CWT(D)$  on an example of the ShB\_500S sampling site; marked dense clusters of cells are typical tracheids of earlywood (solid boundary line) and latewood (dashed boundary line); straight line represents threshold  $k$  for this site; (b) example of tree ring with IADF (decrease in  $D$  in several cells of earlywood); cells where  $CWT/D > k$  are marked with shaded areas; the left shaded area caused by IADF was manually sorted as earlywood. The following  $k$  values have been applied: ShB\_1300N–0.14; ShB\_900N–0.09; ShB\_900S–0.12; ShB\_500S–0.10; MIN\_300–0.11.

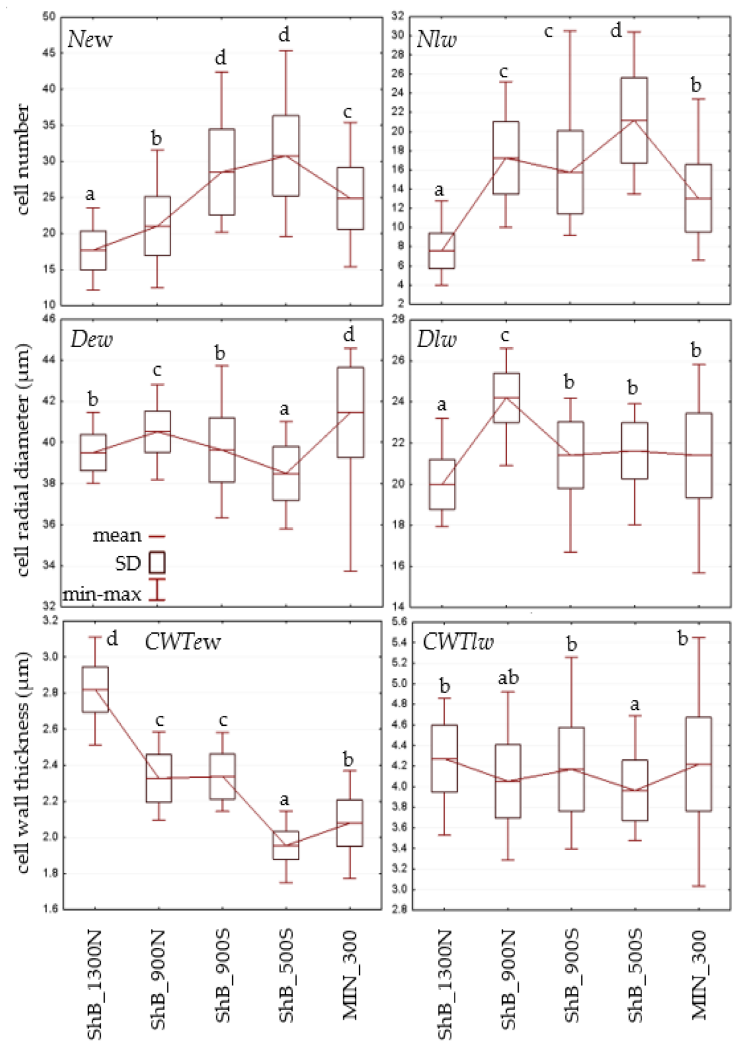


**Figure A4.** Ranges of variation for Scots pine wood anatomical traits: mean values, standard deviations *SD*, and full range from minimum to maximum values. Different letters indicate differences significant at  $p = 0.05$  (ANOVA).

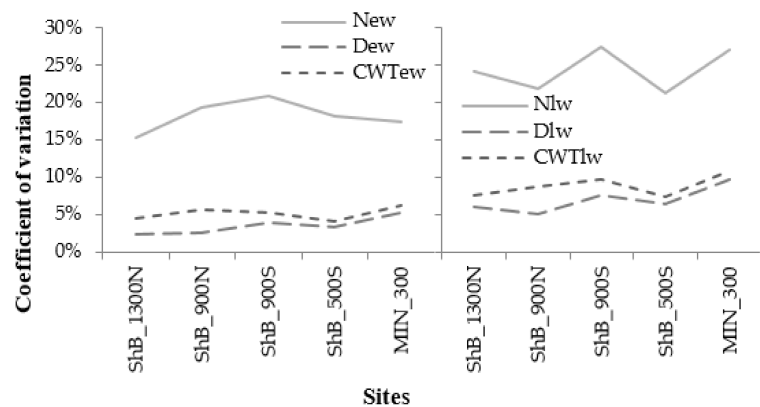


**Figure A5.** Coefficient of variation ( $var = SD/mean \cdot 100\%$ ) values for the anatomical site chronologies of earlywood (left panel) and latewood (right panel).

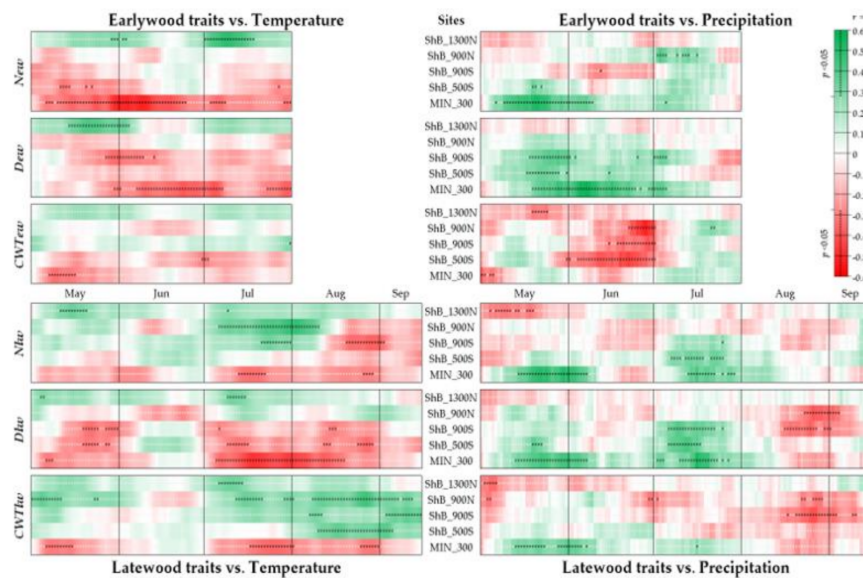


**Figure A6.** Correlations between earlywood (top) and latewood (bottom) cell anatomical chronologies with the 21-day moving series of mean temperature (left) and precipitation (right). Strength of positive (green) and negative (red) correlations is represented by intensity gradient of color, see the legend. Correlations significant at  $p < 0.05$  are marked with dots.

## References

- Esper, J.; Frank, D.C.; Luterbacher, J. On selected issues and challenges in dendroclimatology. In *A Changing World: Challenges for Landscape Research*; Kienast, F., Wildi, O., Ghosh, S., Eds.; Springer: Dordrecht, The Netherlands, 2007; pp. 113–132. [\[CrossRef\]](#)
- Gärtner, H.; Cherubini, P.; Fonti, P.; von Arx, G.; Schneider, L.; Nievergelt, D.; Verstege, A.; Bast, A.; Schweingruber, F.H.; Büntgen, U. A technical perspective in modern tree-ring research—How to overcome dendroecological and wood anatomical challenges. *J. Vis. Exp.* **2015**, *97*, e52337. [\[CrossRef\]](#)
- Fritts, H.C. *Tree Rings and Climate*; Academic Press: London, UK, 1976.
- Vaganov, E.A.; Hughes, M.K.; Shashkin, A.V. *Growth Dynamics of Conifer Tree Rings: Images of Past and Future Environments*; Springer: Berlin, Germany, 2006. [\[CrossRef\]](#)
- Kononov, Y.M.; Friedrich, M.; Boettger, T. Regional summer temperature reconstruction in the Khibiny low mountains (Kola peninsula, NW Russia) by means of tree-ring width during the last four centuries. *Arct. Antarct. Alp. Res.* **2009**, *41*, 460–468. [\[CrossRef\]](#)
- Keyimu, M.; Li, Z.; Zhang, G.; Fan, Z.; Wang, X.; Fu, B. Tree ring-based minimum temperature reconstruction in the central Hengduan Mountains, China. *Theor. Appl. Climatol.* **2020**, *141*, 359–370. [\[CrossRef\]](#)
- D'Arrigo, R.D.; Jacoby, G.C.; Free, R.M. Tree-ring width and maximum latewood density at the North American tree line: Parameters of climatic change. *Can. J. For. Res.* **1992**, *22*, 1290–1296. [\[CrossRef\]](#)
- Gindl, W.; Grabner, M.; Wimmer, R. The influence of temperature on latewood lignin content in treeline Norway spruce compared with maximum density and ring width. *Trees* **2000**, *14*, 409–414. [\[CrossRef\]](#)
- Lebourgeois, F. Climatic signals in earlywood, latewood and total ring width of Corsican pine from western France. *Ann. For. Sci.* **2000**, *57*, 155–164. [\[CrossRef\]](#)
- Meko, D.M.; Baisan, C.H. Pilot study of latewood-width of conifers as an indicator of variability of summer rainfall in the North American monsoon region. *Int. J. Climatol.* **2001**, *21*, 697–708. [\[CrossRef\]](#)
- Fonti, P.; von Arx, G.; García-González, I.; Eilmann, B.; Sass-Klaassen, U.; Gärtner, H.; Eckstein, D. Studying global change through investigation of the plastic responses of xylem anatomy in tree rings. *New Phytol.* **2010**, *185*, 42–53. [\[CrossRef\]](#)
- von Arx, G.; Crivellaro, A.; Prendin, A.L.; Čufar, K.; Carrer, M. Quantitative wood anatomy—practical guidelines. *Front. Plant Sci.* **2016**, *7*, 781. [\[CrossRef\]](#)

13. Fonti, P.; Bryukhanova, M.; Myglan, V.; Naumova, O.; Kirdyanov, A.; Vaganov, E. Temperature-induced responses of xylem structure of *Larix sibirica* Ldb. (*Pinaceae*) from Russian Altay. *Am. J. Bot.* **2013**, *100*, 1332–1343. [[CrossRef](#)]
14. Castagneri, D.; Fonti, P.; von Arx, G.; Carrer, M. How does climate influence xylem morphogenesis over the growing season? Insights from long-term intra-ring anatomy in *Picea abies*. *Ann. Bot.* **2017**, *19*, 1011–1020. [[CrossRef](#)]
15. Carrer, M.; Castagneri, D.; Prendin, A.L.; Petit, G.; von Arx, G. Retrospective analysis of wood anatomical traits reveals a recent extension in tree cambial activity in two high-elevation conifers. *Front. Plant Sci.* **2017**, *8*, 737. [[CrossRef](#)] [[PubMed](#)]
16. Deslauriers, A.; Morin, H. Intra-annual tracheid production in balsam fir stems and the effect of meteorological variables. *Trees* **2005**, *19*, 402–408. [[CrossRef](#)]
17. Ziaco, E.; Liang, E. New perspectives on sub-seasonal xylem anatomical responses to climatic variability. *Trees* **2019**, *33*, 973–975. [[CrossRef](#)]
18. Rathgeber, C.B.; Cuny, H.E.; Fonti, P. Biological basis of tree-ring formation: A crash course. *Front. Plant Sci.* **2016**, *7*, 734. [[CrossRef](#)] [[PubMed](#)]
19. De Micco, V.; Carrer, M.; Rathgeber, C.B.; Camarero, J.J.; Voltas, J.; Cherubini, P.; Battipaglia, G. From xylogenesis to tree rings: Wood traits to investigate tree response to environmental changes. *IAWA J.* **2019**, *40*, 155–182. [[CrossRef](#)]
20. Cuny, H.E.; Rathgeber, C.B.K.; Frank, D.; Fonti, P.; Mäkinen, H.; Prislán, P.; Rossi, S.; Martínez del Castillo, E.; Campelo, F.; Vavrčík, H.; et al. Woody biomass production lags stem-girth increase by over one month in coniferous forests. *Nat. Plants* **2015**, *1*, 15160. [[CrossRef](#)]
21. Hacke, U.G.; Lachenbruch, B.; Pittermann, J.; Mayr, S.; Domec, J.C.; Schulte, P.J. The hydraulic architecture of conifers. In *Functional and Ecological Xylem Anatomy*; Hacke, U., Ed.; Springer: Cham, Switzerland, 2015; pp. 39–75. [[CrossRef](#)]
22. Arzac, A.; Babushkina, E.A.; Fonti, P.; Slobodchikova, V.; Sviderskaya, I.V.; Vaganov, E.A. Evidences of wider latewood in *Pinus sylvestris* from a forest-steppe of Southern Siberia. *Dendrochronologia* **2018**, *49*, 1–8. [[CrossRef](#)]
23. Rossi, S.; Deslauriers, A.; Anfodillo, T. Assessment of cambial activity and xylogenesis by microsampling tree species: An example at the Alpine timberline. *IAWA J.* **2006**, *27*, 383–394. [[CrossRef](#)]
24. Shorohova, E.; Kneeshaw, D.; Kuuluvainen, T.; Gauthier, S. Variability and dynamics of old-growth forests in the circumboreal zone: Implications for conservation, restoration and management. *Silva Fenn.* **2011**, *45*, 785–806. [[CrossRef](#)]
25. Houston Durrant, T.; de Rigo, D.; Caudullo, G. *Pinus sylvestris* in Europe: Distribution, habitat, usage and threats. In *European Atlas of Forest Tree Species*; San-Miguel-Ayanz, J., de Rigo, D., Caudullo, G., Houston Durrant, T., Mauri, A., Eds.; Publication Office of the European Union: Luxembourg, 2016; pp. 132–133.
26. Grissino-Mayer, H.D. An updated list of species used in tree-ring research. *Tree-Ring Bull.* **1993**, *53*, 17–43.
27. Alisov, B.P. *Climate of the USSR*; Moscow State University: Moscow, Russia, 1956. (In Russian)
28. Polikarpov, N.P.; Nazimova, D.I. The dark coniferous forests of the northern part of the west Siberian mountains. *For. Res. For. Sib.* **1936**, *57*, 103–147. (In Russian)
29. Cook, E.R.; Kairiukstis, L.A. (Eds.) *Methods of Dendrochronology: Application in Environmental Sciences*; Kluwer Academic Publishers: Dordrecht, The Netherlands, 1990. [[CrossRef](#)]
30. Carrer, M.; von Arx, G.; Castagneri, D.; Petit, G. Distilling allometric and environmental information from time series of conduit size: The standardization issue and its relationship to tree hydraulic architecture. *Tree Physiol.* **2015**, *35*, 27–33. [[CrossRef](#)] [[PubMed](#)]
31. Silkin, P.P. *Methods of Multiparameter Analysis of Conifers Tree-Rings Structure*; Siberian Federal University: Krasnoyarsk, Russia, 2010. (In Russian)
32. Seo, J.W.; Smiljanić, M.; Wilmking, M. Optimizing cell-anatomical chronologies of Scots pine by stepwise increasing the number of radial tracheid rows included—Case study based on three Scandinavian sites. *Dendrochronologia* **2014**, *32*, 205–209. [[CrossRef](#)]
33. Belokopytova, L.V.; Babushkina, E.A.; Zhirnova, D.F.; Panyushkina, I.P.; Vaganov, E.A. Pine and larch tracheids capture seasonal variations of climatic signal at moisture-limited sites. *Trees* **2019**, *33*, 227–242. [[CrossRef](#)]

34. Vaganov, E.A. The tracheidogram method in tree-ring analysis and its application. In *Methods of dendrochronology. Application in Environmental Sciences*; Cook, E.R., Kairiukstis, L.A., Eds.; Kluwer Academic Publishers: Dordrecht, The Netherlands, 1990; pp. 63–75. [\[CrossRef\]](#)
35. Bryukhanova, M.; Fonti, P. Xylem plasticity allows rapid hydraulic adjustment to annual climatic variability. *Trees* **2013**, *27*, 485–496. [\[CrossRef\]](#)
36. Anfodillo, T.; Carraro, V.; Carrer, M.; Fior, C.; Rossi, S. Convergent tapering of xylem conduits in different woody species. *New Phytol.* **2006**, *169*, 279–290. [\[CrossRef\]](#) [\[PubMed\]](#)
37. Meinzer, F.C.; Lachenbruch, B.; Dawson, T.E. *Size- and Age-Related Changes in Tree Structure and Function*; Springer: Dordrecht, The Netherlands, 2011. [\[CrossRef\]](#)
38. Carteni, F.; Deslauriers, A.; Rossi, S.; Morin, H.; De Micco, V.; Mazzoleni, S.; Giannino, F. The physiological mechanisms behind the earlywood-to-latewood transition: A process-based modeling approach. *Front. Plant Sci.* **2018**, *9*, 1053. [\[CrossRef\]](#)
39. Ziaco, E.; Biondi, F.; Heinrich, I. Wood cellular dendroclimatology: Testing new proxies in Great Basin bristlecone pine. *Front. Plant Sci.* **2016**, *7*, 1602. [\[CrossRef\]](#)
40. Martínez-Sancho, E.; Dorado-Liñán, I.; Hacke, U.G.; Seidel, H.; Menzel, A. Contrasting hydraulic architectures of Scots pine and sessile oak at their southernmost distribution limits. *Front. Plant Sci.* **2017**, *8*, 598. [\[CrossRef\]](#)
41. Kalinina, E.V.; Knorre, A.A.; Fonti, M.V.; Vaganov, E.A. Seasonal formation of tree rings in Siberian larch and Scots pine in the southern taiga of Central Siberia. *Russ. J. Ecol.* **2019**, *50*, 227–233. [\[CrossRef\]](#)
42. Prendin, A.L.; Petit, G.; Fonti, P.; Rixen, C.; Dawes, M.A.; von Arx, G. Axial xylem architecture of *Larix decidua* exposed to CO<sub>2</sub> enrichment and soil warming at the treeline. *Funct. Ecol.* **2018**, *32*, 273–287. [\[CrossRef\]](#)
43. Hacke, U.G.; Sperry, J.S. Functional and ecological xylem anatomy. *Perspect. Plant Ecol. Evol. Syst.* **2001**, *4*, 97–115. [\[CrossRef\]](#)
44. Björklund, J.; Seftigen, K.; Schweingruber, F.; Fonti, P.; von Arx, G.; Bryukhanova, M.V.; Cuny, H.E.; Carrer, M.; Castagneri, D.; Frank, D.C. Cell size and wall dimensions drive distinct variability of earlywood and latewood density in Northern Hemisphere conifers. *New Phytol.* **2017**, *216*, 728–740. [\[CrossRef\]](#) [\[PubMed\]](#)
45. Vieira, J.; Carvalho, A.; Campelo, F. Tree growth under climate change: Evidence from xylogenesis timings and kinetics. *Front. Plant Sci.* **2020**, *11*, 90. [\[CrossRef\]](#) [\[PubMed\]](#)
46. Proseus, T.E.; Boyer, J.S. Turgor pressure moves polysaccharides into growing cell walls of *Chara corallina*. *Ann. Bot.* **2005**, *95*, 967–979. [\[CrossRef\]](#) [\[PubMed\]](#)
47. Ziaco, E.; Truettner, C.; Biondi, F.; Bullock, S. Moisture-driven xylogenesis in *Pinus ponderosa* from a Mojave Desert mountain reveals high phenological plasticity. *Plant Cell Environ.* **2018**, *41*, 823–836. [\[CrossRef\]](#) [\[PubMed\]](#)
48. Cabon, A.; Peters, R.L.; Fonti, P.; Martínez-Vilalta, J.; De Cáceres, M. Temperature and water potential co-limit stem cambial activity along a steep elevational gradient. *New Phytol.* **2020**, *226*, 1325–1340. [\[CrossRef\]](#)
49. Peters, R.; Steppe, K.; Cuny, H.; de Pauw, D.; Frank, D.F.C.; Schaub, M.; Rathgeber, C.B.K.; Cabon, A.; Fonti, P. Turgor—A limiting factor for radial growth in mature conifers along an elevational gradient. *New Phytol.* **2020**. [\[CrossRef\]](#)
50. Camarero, J.; Olano, J.M.; Parras, A. Plastic bimodal xylogenesis in conifers from continental Mediterranean climates. *New Phytol.* **2010**, *185*, 471–480. [\[CrossRef\]](#)
51. Campelo, F.; Gutiérrez, E.; Ribas, M.; Sánchez-Salguero, R.; Nabais, C.; Camarero, J. The facultative bimodal growth pattern in *Quercus ilex*—A simple model to predict sub-seasonal and inter-annual growth. *Dendrochronologia* **2018**, *49*, 77–88. [\[CrossRef\]](#)
52. Schweingruber, F.H.; Bartholin, T.; Schär, E.; Briffa, K.R. Radiodensitometric-dendroclimatological conifer chronologies from Lapland (Scandinavia) and the Alps (Switzerland). *Boreas* **1988**, *17*, 559–566. [\[CrossRef\]](#)
53. Briffa, K.R.; Jones, P.D.; Schweingruber, F.H. Tree-ring density reconstructions of summer temperature patterns across western North America since 1600. *J. Clim.* **1992**, *5*, 735–754. [\[CrossRef\]](#)

**Publisher’s Note:** MDPI stays neutral with regard to jurisdictional claims in published maps and institutional affiliations.



© 2020 by the authors. Licensee MDPI, Basel, Switzerland. This article is an open access article distributed under the terms and conditions of the Creative Commons Attribution (CC BY) license (<http://creativecommons.org/licenses/by/4.0/>).